Journal of
Marine Science and Engineering

MDPI

Article

Cooperative Maritime Search of Multi-Ship Based on Improved Robust Line-of-Sight Guidance

Weili Guo, Cheng Liu * and Ting Sun

Navigation College, Dalian Maritime University, Dalian 116026, China; g_wl@dlmu.edu.cn (W.G.); tstingsun@dlmu.edu.cn (T.S.)
* Correspondence: chengliu@dlmu.edu.cn

Abstract: In this paper, an improved robust line-of-sight (RLOS) guidance-based fuzzy sliding mode controller is presented to control underactuated ships to conduct the cooperative maritime search operation under the presented improved creeping line search method. First, considering that the ship cannot perform turning with corners, an improved creeping line search method is presented by integrating the Bezier method into the traditional creeping line search method to smooth the transition points with corners and employing the cubic spline interpolation method to generate continuous reference paths. Second, an improved RLOS guidance method is presented for the first time by exploring the idea of robust adaptive control to mitigate the chattering effect of the RLOS guidance. Third, the fuzzy logic system with approximate ability is integrated into the design of sliding mode controller to handle unknown nonlinear model dynamics and environmental disturbances. Finally, an improved RLOS guidance-based fuzzy sliding mode controller is presented. The closed-loop stability is guaranteed by the Lyapunov theorem. Comparative simulations are conducted to illustrate the advantages and verify the effectiveness of the presented method.

Keywords: improved robust line-of-sight; cooperative maritime search; fuzzy logic system; path planning

Citation: Guo, W.; Liu, C.; Sun, T. Cooperative Maritime Search of Multi-Ship Based on Improved Robust Line-of-Sight Guidance. *J. Mar. Sci. Eng.* **2024**, *12*, 105. https://doi.org/10.3390/jmse12010105

Academic Editor: Marco Cococcioni

Received: 13 December 2023
Revised: 30 December 2023
Accepted: 2 January 2024
Published: 5 January 2024

1. Introduction

Maritime transportation is the main role of cargo transportation among countries, and more than 90% of global trade, which is worth billions of dollars, is carried by ships [1]. The increasing crowded channels and complex marine environment would unfortunately lead to a certain number of maritime accidents. Although a great number of efforts have been made to reduce the maritime accidents, e.g., sea traffic monitoring, navigation safety countermeasures assessment, and scientific ship management system [1,2], maritime accidents still happen. Thus, it is of great significance to conduct maritime search and rescue operations for saving human life within stringent time. The maritime search is the premise of maritime rescue [3–5]. Compared with an individual maritime search operation [3,4], the cooperative maritime search can save the search time efficiently. Thus, autonomous control for cooperative maritime search of multiple underactuated ships is studied herein.

Maritime search is an operation which utilizes available information and facilities to locate people in distress. In practice, the positions of people and ships in distress are time-varying due to the influence of maritime environment; thus, planning an efficient search path for ships is essential. There are two typical path planning methods. One is point-to-point path planning, and the other is coverage path planning [5]. The point-to-point method requires the start point and the end point to be available, and the objective of this method is to obtain the shortest search path. Nevertheless, the information about accurate positions of maritime accidents and people in distress is difficult to be determined. In this situation, an effective method is to determine a search area based on the information about the possible positions of maritime accidents, and then design the optimal search path for ships to cover the whole search area. The above process is coverage search, and the coverage search method includes, e.g., creeping line search, parallel track search, expanding square search, and sector search [5,6]. Compared with the point-to-point search method, the coverage search method is more suitable to the scenario in which the information about positions of maritime accidents is uncertain. Moreover, compared with the individual maritime search operation [3,4], the cooperative maritime search, which is conducted by multiple ships, is more efficient. To sum up, the autonomous control of cooperative maritime search based on coverage search method is studied herein.

The creeping line search method [6] has transition points with corners, which is impossible for ships to follow due to the given maneuverability; thus, in order to obtain a smooth reference path, it is of significance to study path planning for cooperative maritime search operation. The Bezier curve can be used to generate a smooth curve based on control points [7,8]; however, the results are in discontinuous form, and cannot be used as a reference path for a control system, which requires the second derivative. In order to handle this problem, the cubic spline interpolation [9,10], which can generate a continuous reference signal based on discontinuous points, is employed in this paper. To sum up, an improved creeping line search method is presented for cooperative maritime search operation for the first time by integrating the cubic spline interpolation into the Bezier curve. Compared with the traditional creeping line search method with transition points with corners [6], which is impossible for underactuated ships to follow, the presented improved creeping line search method generates smooth reference path.

The underactuated ship, i.e., the ship without a sway actuator, is the general configuration, and it attracts intense interest in research because of theoretical challenges and wide applications [11–20]. The line-of-sight (LOS) guidance [11] has been employed widely as a useful method for path following of underactuated ships; however, the influence of the sideslip angle and kinematic uncertainty are ignored. Many researchers explored the LOS guidance method in depth and improved it, see Table 1. The kinematic discrepancy between the ship and its three-degree-of-freedom (3-DoF) mathematical model is almost ignored in previous studies [12,13,16,21]. The robust LOS (RLOS) method was presented to compensate kinematic uncertainty by exploring the idea of sliding mode in [18]; however, the chattering effect was ignored. Thus, it is of significance to study the idea of chattering-free sliding mode further. The idea of robust adaptive control [22] is employed to reduce the chattering effect of RLOS; then, the improved RLOS is presented in this paper.

Table 1. The characteristics of previous work about LOS guidance.

Reference	Advantage	Shortcoming
[11]	It provides a simple method to handle the path following problem of underactuated ships.	It ignores the influence of the sideslip angel and kinematic uncertainty.
[12,21]	An integral term is used to alleviate the influence of the sideslip angel.	It cannot handle the time-varying sideslip angle and ignores the kinematic uncertainty.
[13,16]	A reduced-order extended state observer is employed to identify the time-varying sideslip angle.	It ignores the kinematic uncertainty.
[18]	A robust term is employed to compensate the kinematic uncertainty.	It ignores the influence of the sideslip angle and exists the chattering effect.

Sliding mode control [23,24] has the advantages of robustness, and it can be employed to control ships to perform path following [16,25–28]. In order to control underactuated ships to perform path following, an integral LOS guidance-based sliding mode controller was presented [28]; a sliding mode controller based on an improved extended state observe-based LOS guidance was presented in [16]; and an efficient LOS guidance-based sliding mode controller was presented by employing an event-triggered strategy to reduce trigger time [25]. Nevertheless, the above studies are concentrated on an individual ship. The improved RLOS guidance-based sliding mode controller is presented for cooperative maritime search operation for the first time in this paper. Considering that the unknown model dynamics and time-varying disturbances always exist, the fuzzy logic system (FLS) [29] with approximate ability can be integrated into the presented controller to approximate the nonlinear function [30–33]. To sum up, an improved RLOS guidance-based fuzzy sliding mode controller is presented for the first time for cooperative maritime search of multiple underactuated ships.

The contributions of this paper can be summarized as follows.

(1) In previous work [3,4], the maritime search has been conducted by an individual ship. Compared with an individual maritime search operation [3,4], the cooperative maritime search based on the improved creeping line search method is presented in this paper, which is more efficient within stringent time.
(2) Compared with the traditional creeping line search method [6] with transition points with corners, which is impossible for ships to track, the presented improved creeping line search method smooths the transition points with corners based on the Bezier curve; then, a smooth reference path can be obtained.
(3) The RLOS guidance method [18] compensates the kinematic uncertainty by exploring the idea of sliding mode; however, the chattering effect always exists. Considering the shortcoming of the RLOS guidance method, an improved RLOS guidance method with less chattering effect is presented in this paper for the first time by employing the idea of robust adaptive control.
(4) Considering the unknown nonlinear model dynamics and time-varying disturbances, the FLS is incorporated into the design of the controller to approximate the unknown nonlinear functions; then, the improved RLOS guidance-based fuzzy sliding mode controller is presented for the cooperative maritime search operation.

The rest of this paper is organized as follows. Section 2 states mathematical model, search path planning method, improved RLOS guidance, fuzzy logical system, and problem formulation. Section 3 states the design of controller. Section 4 conducts two simulations to validate the presented method. Section 5 gives the conclusions.

2. Preliminaries and Problem Formulation

2.1. Mathematical Model of Underactuated Ships

The 3-DoF horizontal dynamics of the i-th ship [20] can be written as

$$\begin{aligned} \dot{x}_i &= u_i \cos\psi_i - v_i \sin\psi_i \\ \dot{y}_i &= u_i \sin\psi_i + v_i \cos\psi_i \\ \dot{\psi}_i &= r_i \end{aligned} \tag{1}$$

$$\begin{aligned} \dot{u}_i &= \tfrac{m_{i22}}{m_{i11}} v_i r_i - \tfrac{d_{iu}}{m_{i11}} u_i - \tfrac{d_{iu2}}{m_{i11}} |u_i| u_i - \tfrac{d_{iu3}}{m_{i11}} u_i^3 + \tfrac{1}{m_{i11}} \tau_{iu} + \tfrac{1}{m_{i11}} \tau_{iwu} \\ \dot{v}_i &= -\tfrac{m_{i11}}{m_{i22}} u_i r_i - \tfrac{d_{iv}}{m_{i22}} v_i - \tfrac{d_{iv2}}{m_{i22}} |v_i| v_i - \tfrac{d_{iv3}}{m_{i22}} v_i^3 + \tfrac{1}{m_{i22}} \tau_{iwv} \\ \dot{r}_i &= \tfrac{m_{i11} - m_{i22}}{m_{i33}} u_i v_i - \tfrac{d_{ir}}{m_{i33}} r_i - \tfrac{d_{ir2}}{m_{i33}} |r_i| r_i - \tfrac{d_{ir3}}{m_{i33}} r_i^3 + \tfrac{1}{m_{i33}} \tau_{ir} + \tfrac{1}{m_{i33}} \tau_{iwr} \end{aligned} \tag{2}$$

where (x_i, y_i) describes the position of ships, and ψ_i is the yaw angle; u_i, v_i, and r_i denote velocities of surge, sway, and yaw rate. The positive constant terms m_{i11}, m_{i22}, and m_{i33} represent the ship inertia including added mass. The terms d_{iu}, d_{iu2},d_{iu3}, d_{iv}, d_{iv2}, d_{iv3}, d_{ir}, d_{ir2}, and d_{ir3} denote the hydrodynamic damping in surge, sway, and yaw. τ_{iwu}, τ_{iwv}, and τ_{iwr} are environmental disturbances produced by current, wave, and wind. The surge force τ_{iu} and the yaw moment τ_{ir} are available controllers.

2.2. A Novel Path Planning Method

The traditional creeping line search method is one of classical coverage methods, but it has transition points with corners. It is impossible for ships to perform the turning with corners, which poses challenges in maritime search operation. A novel path planning method for cooperative maritime search operation is presented based on the improved creeping line search method using the Bezier curve and the cubic spline interpolation in this paper. The Bezier curve is widely used in various areas to produce a smooth curve based on the given control points [7,8]; however, the results of the Bezier curve are in a discontinuous form, which cannot be used as a reference path for a control system directly, which requires the second derivative. Thus, the cubic spline interpolation is introduced to connect these discontinuous reference points [10]; then, a smooth reference path can be presented herein. The details are given as follows.

2.2.1. Improved Creeping Line Search Method

Creeping line search is a traditional coverage search method, which aims to cover the whole area [6]. Compared with an individual search operation, cooperative search can effectively save search time. Then, the cooperative creeping line search for multi-ship is introduced herein, and the three-ship cooperative search is taken as an illustrated example, see Figure 1. W is the sweep width, and it also can be denoted as the distance between adjacent paths [4]. The value of W can be obtained from [6].

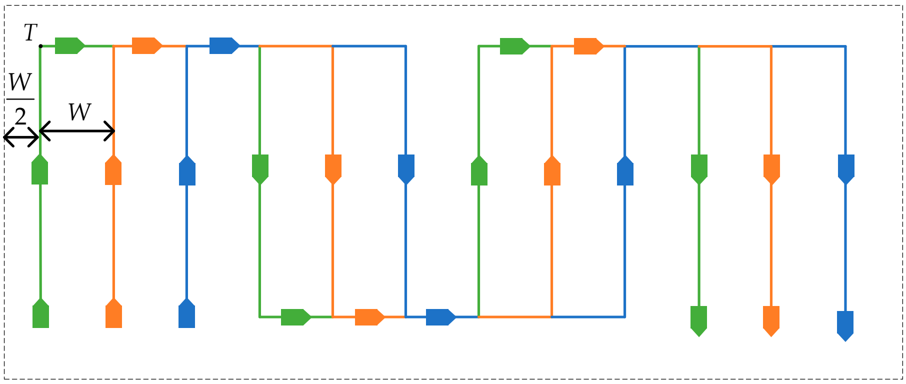

Figure 1. Cooperative creeping line search method.

Nevertheless, the traditional creeping line search method has transition points with corners (e.g., T in Figure 1), which is impossible for ships to follow due to their given maneuverability; thus, in order to obtain a smooth reference path, researching the path planning method is significant. The Bezier curve, which is used in various areas to produce a curve based on the given control points, is considered herein [7,8]. It can be given as follows

$$R(\alpha) = \sum_{\varsigma=0}^{n} I_{\varsigma} \Gamma_{\varsigma}^{n}(\alpha) \tag{3}$$

where α is a parameter, which satisfies $\alpha \in [0,1]$, and I_{ς} ($\varsigma = 0, 1, \ldots, n$) are control points. $\Gamma_{\varsigma}^{n}(\alpha)$ is a Bernstein polynomial

$$\Gamma_{\varsigma}^{n}(\alpha) = C_{n}^{\varsigma} \alpha^{\varsigma} (1-\alpha)^{n-\varsigma} \tag{4}$$

where $C_{n}^{\varsigma} = \frac{n!}{\varsigma!(n-\varsigma)!}$.

Then, an improved creeping line search method is presented by incorporating the Bezier curve into the traditional creeping line search method, i.e., a curve segment between two lines (e.g., the curve segment between $P_{100}P_{110}$ and $P_{112}P_{120}$ in Figure 2), which is produced by the Bezier curve, and is employed to circumvent the transition points. The Bezier curve of three degrees is employed herein

$$B_{ig}(\alpha_{ig}) = (1-\alpha_{ig})^{2} P_{ig0} + 2\alpha_{ig}(1-\alpha_{ig}) P_{ig1} + \alpha_{ig}^{2} P_{ig2} \tag{5}$$

where P_{igt} are used to produce the reference points of the g-th ($g = 1, 2, \ldots, M$) curve segment of the i-th ($i = 1, 2, \ldots, K$) ship, and $t = 0, 1, 2$ are three control points of the Bezier curve. In order to guarantee the distance between adjacent paths to be equal to W, the control points of the i-ship can be designed as $P_{igt} = [x_{1gt}, y_{1gt} + (i-1)W]$, e.g., $P_{1gt} = (x_{1gt}, y_{1gt})$ is a control point of the first ship. Then, an ordered series of reference points of each curve segment can be obtained according to Equation (5). Considering the start point $P_{i00} = \left(x^b_{i0}, y^b_{i0}\right)$ and the end point $P_{i(M+1)0} = \left(x^b_{i(MN+1)}, y^b_{i(MN+1)}\right)$, the set of reference points of the i-ship can be expressed as follows

$$\Pi_i = \left\{ \left(x^b_{i0}, y^b_{i0}\right), \left(x^b_{i1}, y^b_{i1}\right), \ldots, \left(x^b_{i(MN+1)}, y^b_{i(MN+1)}\right) \right\} \tag{6}$$

where N is the number of reference points of each curve segment.

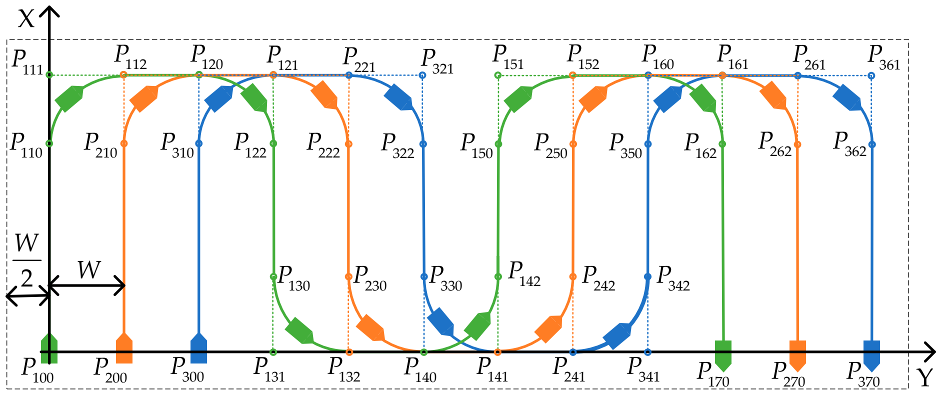

Figure 2. An improved creeping line search for cooperative search operation.

2.2.2. Cubic Spline Interpolation

The set of reference points Π_i can be obtained based on the above Bezier algorithm; however, these discontinuous reference points cannot be used as a reference path for control system directly. Thus, the cubic spline interpolation is introduced to obtain a differentiable reference path herein.

The cubic polynomial can be expressed as follows [10]

$$\begin{aligned} x_{ip}(\zeta_i) &= a_{i3}\zeta_i^3 + a_{i2}\zeta_i^2 + a_{i1}\zeta_i + a_{i0} \\ y_{ip}(\zeta_i) &= b_{i3}\zeta_i^3 + b_{i2}\zeta_i^2 + b_{i1}\zeta_i + b_{i0} \end{aligned} \tag{7}$$

where $a_i = [a_{i3}, a_{i2}, a_{i1}, a_{i0}]^T$ and $b_i = [b_{i3}, b_{i2}, b_{i1}, b_{i0}]^T$ can be computed based on the obtained set of reference points Π_i and the cubic spline interpolation [9,10]. ζ_i is a parametric variable. Eventually, a differentiable reference path $[x_{ip}(\zeta_i), y_{ip}(\zeta_i)]$ is obtained based on the Bezier curve and cubic spline interpolation.

2.3. Improved RLOS Guidance

LOS guidance has been proved as a useful guidance method for path following of underactuated ships [12,13,16,18]. The desired yaw angle ψ_{id} generated by the guidance system is employed to steer the ships to track reference paths, which lowers the dimension of control outputs. A geometrical illustration of LOS guidance can be seen in Figure 3.

Define a path-tangential reference frame at $[x_{ip}(\zeta_i), y_{ip}(\zeta_i)]$. This path-tangential angle ϕ_i can be obtained as follows [11]

$$\phi_i(\zeta_i) = \arctan\left[\frac{y'_{ip}(\zeta_i)}{x'_{ip}(\zeta_i)}\right] \tag{8}$$

where $x'_{ip}(\zeta_i) = \frac{\partial x_{ip}}{\partial \zeta_i}$, $y'_{ip}(\zeta_i) = \frac{\partial y_{ip}}{\partial \zeta_i}$.

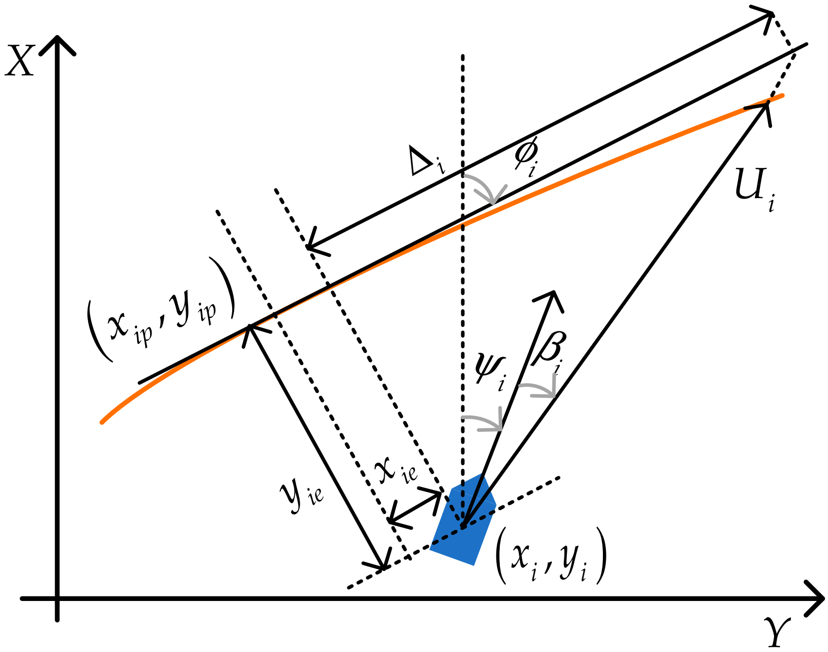

Figure 3. The geometry of LOS guidance.

The guidance system is

$$\begin{bmatrix} \dot{x}_{id}(\zeta_i) \\ \dot{y}_{id}(\zeta_i) \end{bmatrix} = \begin{bmatrix} \cos\phi_i & -\sin\phi_i \\ \sin\phi_i & \cos\phi_i \end{bmatrix} \begin{bmatrix} U_{ip} \\ 0 \end{bmatrix} \tag{9}$$

where U_{ip} is virtual input, and $\dot{\zeta}_i = \frac{U_{ip}}{\sqrt{x'_{ip}{}^2(\zeta_i)+y'_{ip}{}^2(\zeta_i)}}$.

The along-track error and cross-track error can be defined as

$$\begin{bmatrix} x_{ie} \\ y_{ie} \end{bmatrix} = \begin{bmatrix} \cos\phi_i & -\sin\phi_i \\ \sin\phi_i & \cos\phi_i \end{bmatrix}^T \begin{bmatrix} x_i - x_{id} \\ y_i - y_{id} \end{bmatrix} \tag{10}$$

Differentiate Equation (10), it has

$$\begin{aligned} \dot{x}_{ie} &= U_i\cos(\psi_i - \phi_i + \beta_i) - U_{ip} + \dot{\phi}_i y_{ie} + \xi_i \\ \dot{y}_{ie} &= U_i\sin(\psi_i - \phi_i + \beta_i) - \dot{\phi}_i x_{ie} \end{aligned} \tag{11}$$

where $U_i = \sqrt{u_i^2 + v_i^2}$ is the speed of ships, $\beta_i = \arctan\left(\frac{v_i}{u_i}\right)$ is the sideslip angle, and ξ_i denotes the kinematic discrepancy between the ship and its 3-DoF model. The discrepancy is assumed to be bounded, and it satisfies $|\xi_i| \leq \sigma_i$, where σ_i is a positive constant.

The desired yaw angle is designed as follows [11]

$$\psi_{id} = \phi_i - \arctan\left(\frac{y_{ie}}{\Delta_i}\right) - \beta_i \tag{12}$$

where Δ_i is the lookahead distance. Then, Equation (11) can be rewritten as follows

$$\begin{aligned} \dot{x}_{ie} &= U_i\frac{\Delta_i}{\sqrt{\Delta_i^2+y_{ie}^2}} - U_{ip} + \dot{\phi}_i y_{ie} + \xi_i \\ \dot{y}_{ie} &= -U_i\frac{y_{ie}}{\sqrt{\Delta_i^2+y_{ie}^2}} - \dot{\phi}_i x_{ie} \end{aligned} \tag{13}$$

In order to compensate the kinematic discrepancy and stabilize x_{ie}, the virtual input U_{ip} can be designed as

$$U_{ip} = U_i \frac{\Delta_i}{\sqrt{\Delta_i^2 + y_{ie}^2}} + \kappa_{i1} x_{ie} + \kappa_{i2} \tanh\left(\frac{x_{ie}}{\varepsilon_i}\right) \tag{14}$$

where κ_{i1}, κ_{i2}, and ε_i are positive design parameters.

Consider a Lyapunov function

$$V_{iL} = \frac{1}{2} x_{ie}^2 + \frac{1}{2} y_{ie}^2 \geq 0 \tag{15}$$

Differentiate Equation (15), and substitute Equations (13) and (14) into resultant equation

$$\begin{aligned} \dot{V}_{iL} &= x_{ie}\left(U_i \tfrac{\Delta_i}{\sqrt{\Delta_i^2 + y_{ie}^2}} - U_{ip} + \dot{\phi}_i y_{ie} + \xi_i\right) + y_{ie}\left(-U_i \tfrac{y_{ie}}{\sqrt{\Delta_i^2 + y_{ie}^2}} - \dot{\phi}_i x_{ie}\right) \\ &= -\kappa_{i1} x_{ie}^2 - \tfrac{U_i}{\sqrt{\Delta_i^2 + y_{ie}{}^2}} y_{ie}^2 + x_{ie}\xi_i - \kappa_{i2} x_{ie} \tanh\left(\tfrac{x_{ie}}{\varepsilon_i}\right) \\ &\leq \kappa_{i1} x_{ie}^2 - \tfrac{U_i}{\sqrt{\Delta_i^2 + y_{ie}{}^2}} y_{ie}^2 + |x_{ie}\xi_i| - \kappa_{i2} x_{ie} \tanh\left(\tfrac{x_{ie}}{\varepsilon_i}\right) \end{aligned} \tag{16}$$

Because of $|\xi_i| \leq \sigma_i$, Equation (16) satisfies the following inequality

$$\dot{V}_{iL} \leq -\kappa_{i1} x_{ie}^2 - \frac{U_i}{\sqrt{\Delta_i^2 + y_{ie}^2}} y_{ie}^2 + |x_{ie}\sigma_i| - \kappa_{i2} x_{ie} \tanh\left(\frac{x_{ie}}{\varepsilon_i}\right) \tag{17}$$

Let $\kappa_{i2} \geq \sigma_i$, Equation (17) can be written as

$$\dot{V}_{iL} \leq -\kappa_{i1} x_{ie}^2 - \frac{U_i}{\sqrt{\Delta_i^2 + y_{ie}^2}} y_{ie}^2 + \kappa_{i2}\left[|x_{ie}| - x_{ie} \tanh\left(\frac{x_{ie}}{\varepsilon_i}\right)\right] \tag{18}$$

Considering the following inequality

$$0 \leq |x_{ie}| - x_{ie} \tanh\left(\frac{x_{ie}}{\varepsilon_i}\right) \leq \delta\varepsilon_i \tag{19}$$

where δ is a constant that satisfies $\delta = e^{-(\delta+1)}$, i.e., $\delta = 0.2785$ [22].

Equation (18) has

$$\dot{V}_{iL} \leq -\Theta_i V_{iL} + \lambda_i \tag{20}$$

where $\Theta_i = \min\left\{2\kappa_{i1}, \frac{2U_i}{\sqrt{\Delta_i^2 + y_{ie}^2}}\right\}$, and $\lambda_i = \kappa_{i2}\delta\varepsilon_i$.

According to Equations (15) and (20), it concludes that x_{ie} and y_{ie} are bounded.

2.4. Fuzzy Logic System

Considering the unknown nonlinear model dynamics and time-varying disturbances, the FLS, which can be employed to approximate unknown nonlinear function [29–32], is employed in this paper. A group of if-then rules are contained in the knowledge base of the FLS, and they are given as follows [28]

$$R^{(l)}\text{: IF } \chi_1 \text{ is } A_1^l \text{ and } \chi_2 \text{ is } A_2^l \ldots, \text{ and } \chi_n \text{ is } A_n^l, \text{ THEN } \hat{f} \text{ is } D^l \tag{21}$$

where $\chi = [\chi_1, \ldots, \chi_n]^T \subset \mathbb{R}^n$ and $\hat{f} \subset \mathbb{R}$ are input and output variables of the FLS, A_ρ^l and D^l are linguistic terms, which are characterized by fuzzy membership functions $\mu_{A_p^l}(\chi_p)$

and $\mu_{D^l}\left(\hat{f}\right)$. $\rho = 1, 2, \ldots, n$, and n is the number of input variables. $l = 1, 2, \ldots, m$, and m is the number of rules. The membership $\mu_{A_p^l}(\chi_p)$ is defined by Gaussian function [26]

$$\mu_{A_\rho^l}(\chi_\rho) = \exp\left[-\frac{(\chi_\rho - w_l)^2}{2h_l^2}\right] \tag{22}$$

where w_l and h_l are centers and widths of the Gaussian membership function.

The FLS can be described as [28]

$$\hat{f}(\chi) = \frac{\sum\limits_{l=1}^{m} f^{-l}\left[\prod\limits_{\rho=1}^{n} \mu_{A_\rho^l}(\chi_\rho)\right]}{\sum\limits_{l=1}^{m}\left[\prod\limits_{\rho=1}^{n} \mu_{A_\rho^l}(\chi_\rho)\right]} \tag{23}$$

where $f^{-l} = \max\limits_{\hat{f}\in\mathbb{R}} \mu_{D^l}\left(\hat{f}\right)$. Define the fuzzy basis function as

$$\varphi_l(\chi) = \frac{\prod\limits_{\rho=1}^{n} \mu_{A_\rho^l}(\chi_\rho)}{\sum\limits_{l=1}^{m}\prod\limits_{\rho=1}^{n} \mu_{A_\rho^l}(\chi_\rho)} \tag{24}$$

Denoting $\hat{\theta} = \left[f^{-1}, f^{-2}, \ldots, f^{-m}\right]^T$ and $\varphi(\chi) = [\varphi_1(\chi), \varphi_2(\chi), \ldots, \varphi_m(\chi)]^T$; then, Equation (23) can be rewritten as

$$\hat{f}(\chi) = \hat{\theta}^T \varphi(\chi) \tag{25}$$

For a continuous function $f(\chi)$, which is defined on a compact set $\mathbb{N}$, and any constant $\varepsilon_f > 0$, there exists a fuzzy logic system (25) such that [28]

$$\sup_{\chi\in\mathbb{N}}\left|f(\chi) - \hat{f}(\chi)\right| \le \varepsilon_f \tag{26}$$

2.5. Problem Formulation

Cooperative maritime search of multiple underactuated ships based on the improved RLOS guidance-based sliding mode controller is presented herein, and a diagram of information flow is given in Figure 4. First, an improved creeping line search method is presented for the first time for cooperative maritime search by incorporating the Bezier curve into the traditional creeping line search method to circumvent the transition points with corners; then, a smooth reference path can be obtained. Specifically, the Bezier curve is introduced to circumvent transition points with corners in the traditional creeping line search method, and an ordered series of reference points Π_i are obtained; then, the cubic spline interpolation is included to generate differentiable reference paths $\left[x_{ip}(\zeta_i), y_{ip}(\zeta_i)\right]$. Second, the improved RLOS guidance without chattering effect is presented by exploring the idea of robust adaptive control for the first time. By including the improved RLOS, the control output is reduced to the yaw angle, i.e., if the yaw angle can converge to the desired yaw angle ψ_{id}, which is obtained from the improved RLOS guidance, the position of ships can converge to the desired position. Then, the problem of path following of underactuated ships is transformed into heading control problem. Third, the FLS is introduced to approximate unknown nonlinear dynamics and time-varying disturbances. Above all, a fuzzy sliding mode controller based on improved RLOS guidance is presented for the cooperative maritime search operation.

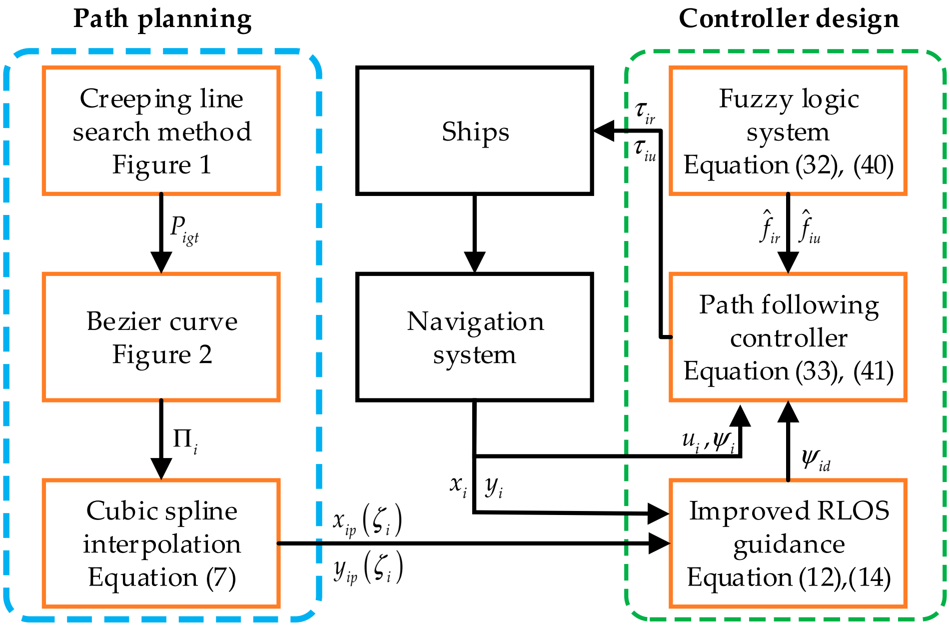

Figure 4. Diagram for cooperative maritime search control of multi-ship based on improved RLOS-guidance.

3. Controller Design

The improved RLOS guidance-based sliding mode controller for the cooperative maritime search operation is designed herein. A desired yaw angle can be obtained from the improved RLOS guidance, see Section 2.3; then, a yaw controller is designed by applying the sliding mode method, and it is used to steer the ship towards the desired search path. Considering the underactuated ships with uncertain dynamics and time-varying disturbances, the FLS is introduced to the design of controller, which is employed to approximate unknown nonlinear model dynamics and time-varying disturbances.

3.1. Yaw Controller

The error between the desired yaw angle and yaw angel can be defined as

$$z_{ir} = \psi_i - \psi_{id} \tag{27}$$

The sliding surface can be designed as

$$s_i = c_{i1} z_{ir} + \dot{z}_{ir} \tag{28}$$

where c_{i1} is a positive parameter. Differentiating Equation (28), it has

$$\dot{s}_i = c_{i1} \dot{z}_{ir} + \dot{r}_i - \ddot{\psi}_{id} \tag{29}$$

$\dot{r}_i$ can be rewritten as

$$\dot{r}_i = f_{ir} + \frac{1}{m_{33}} \tau_{ir} \tag{30}$$

where $f_{ir} = \frac{m_{i11} - m_{i22}}{m_{i33}} u_i v_i - \frac{d_{ir}}{m_{i33}} r_i - \frac{d_{ir2}}{m_{i33}} |r_i| r_i - \frac{d_{ir3}}{m_{i33}} r_i^3 + \frac{1}{m_{i33}} \tau_{iwr}$. The FLS, which is introduced in detail in Section 2.4, is incorporated into the sliding mode controller design to approximate f_{ir}

$$f_{ir} = \theta_{ir}^{*T} \varphi(v_i) + \varepsilon_{ir} \tag{31}$$

where θ_{ir}^* is the ideal parameter vector, $v_i = [u_i, v_i, r_i]^T$, and ε_{ir} is the approximation error. The approximation $\hat{f}_{ir}$ can be obtained based on Equation (25) of the FLS

$$\hat{f}_{ir} = \hat{\theta}_{ir}^T \varphi(v_i) \tag{32}$$

The control input τ_{ir} is designed as follows

$$\tau_{ir} = m_{i33}\left[\ddot{\psi}_{id} - c_{i1}\dot{z}_{ir} - \hat{f}_{ir} - k_i s_i - \eta_{i1} sign(s_i)\right] \tag{33}$$

where k_i and η_{i1} are positive parameters. The adaptive law for $\hat{\theta}_{ir}$ is

$$\dot{\hat{\theta}}_{ir} = \frac{1}{\gamma_{i1}} s_i \varphi(v_i) \tag{34}$$

where γ_{i1} is the positive parameter. Consider the following Lyapunov function

$$V_{ir} = \frac{1}{2}s_i^2 + \frac{1}{2}\gamma_{i1}\widetilde{\theta}_{ir}^T\widetilde{\theta}_{ir} \tag{35}$$

where $\widetilde{\theta}_{ir} = \theta_{ir}^* - \hat{\theta}_{ir}$. Differentiate Equation (35), and substitute Equation (33) and Equation (34) into the resultant equation, it has

$$\begin{aligned} \dot{V}_{ir} &= s_i\dot{s}_i - \gamma_{i1}\widetilde{\theta}_{ir}^T\dot{\hat{\theta}}_{ir} \\ &= s_i\left(f_{ir} - \hat{f}_{ir}\right) - \gamma_{i1}\widetilde{\theta}_{ir}^T\dot{\hat{\theta}}_{ir} - k_i s_i^2 - \eta_{i1}|s_i| \\ &= -k_i s_i^2 - \eta_{i1}|s_i| \leq 0 \end{aligned} \tag{36}$$

According to $V_{ir} \geq 0$ and $\dot{V}_{ir} \leq 0$, it can be concluded that the signals of this closed-loop system are stable.

3.2. Surge Controller

The reference surge velocity is denoted as u_{id}, and the error between the reference surge velocity and surge velocity is defined as

$$z_{iu} = u_i - u_{id} \tag{37}$$

$\dot{u}_i$ can be rewritten as follows

$$\dot{u}_i = f_{iu} + \frac{1}{m_{i11}}\tau_{iu} \tag{38}$$

where $f_{iu} = \frac{m_{i22}}{m_{i11}}v_i r_i - \frac{d_{iu}}{m_{i11}}u_i - \frac{d_{iu2}}{m_{i11}}|u_i|u_i - \frac{d_{iu3}}{m_{i11}}u_i^3 + \frac{1}{m_{i11}}\tau_{iwu}$. The FLS, which is introduced in detail in Section 2.4, is employed to approximate f_{iu}

$$f_{iu} = \theta_{iu}^{*T}\varphi(v_i) + \varepsilon_{iu} \tag{39}$$

where θ_{iu}^* is the ideal parameter vector, and ε_{iu} is the approximation error. The approximate result $\hat{f}_{iu}$ is obtained based on Equation (25) of FLS

$$\hat{f}_{iu} = \hat{\theta}_{iu}^T\varphi(v_i) \tag{40}$$

The control input τ_{iu} is designed as follows

$$\tau_{iu} = m_{i11}\left[-c_{i2}z_{iu} - \hat{f}_{iu} - \eta_{i2} sign(z_{iu})\right] \tag{41}$$

where c_{i2} and η_{i2} are positive parameters. The adaptive law for $\hat{\theta}_{iu}$ is

$$\dot{\hat{\theta}}_{iu} = \frac{1}{\gamma_{i2}} z_{iu}\varphi(v_i) \tag{42}$$

where γ_{i2} is the positive parameter. Define the following Lyapunov function

$$V_{iu} = \frac{1}{2}z_{iu}^2 + \frac{1}{2}\gamma_{i2}\widetilde{\theta}_{iu}^T\widetilde{\theta}_{iu} \tag{43}$$

where $\widetilde{\theta}_{iu} = \theta_{iu}^* - \hat{\theta}_{iu}$. Differentiate Equation (43), and substitute Equation (41) and Equation (42) into the resultant equation, it can be obtained as follows

$$\begin{aligned} \dot{V}_{iu} &= z_{iu}\dot{z}_{iu} - \gamma_{i2}\widetilde{\theta}_{iu}^T\dot{\hat{\theta}}_{iu} \\ &= z_{iu}\left(f_{iu} - \hat{f}_{iu}\right) - c_{i2}z_{iu}^2 - \eta_{i2}|z_{iu}| - \gamma_{i2}\widetilde{\theta}_{iu}^T\dot{\hat{\theta}}_{iu} \\ &= -c_{i2}z_{iu}^2 - \eta_{i2}|z_{iu}| \leq 0 \end{aligned} \tag{44}$$

It can be concluded that the signals of this closed-loop system are stable according to $V_{iu} \geq 0$ and $\dot{V}_{iu} \leq 0$.

4. Simulations

Two cases are conducted to illustrate advantages of the presented improved RLOS guidance-based fuzzy sliding mode controller in this section. The first one gives the performance of the three-ship cooperative maritime search operation based on a novel path planning method, and effectiveness of the fuzzy sliding mode controller based on improved RLOS guidance can be verified. The second one is a comparative case between RLOS guidance and improved RLOS guidance, and it can be conducted to illustrate the advantages of the presented improved RLOS guidance.

The underactuated ships have a length of 38 m, mass of 118×10^3 kg, and the parameters $m_{i11} = 120 \times 10^3$, $m_{i22} = 177.9 \times 10^3$, $m_{i33} = 636 \times 10^5$, $d_{iu} = 251 \times 10^2$, $d_{iv} = 147 \times 10^3$, $d_{ir} = 802 \times 10^4$, $d_{iu2} = 0.2d_{iu}$, $d_{iu3} = 0.1d_{iu}$, $d_{iv2} = 0.2d_{iv}$, $d_{iv3} = 0.1d_{iv}$, $d_{ir2} = 0.2d_{ir}$, and $d_{ir3} = 0.1d_{ir}$ [20]. The time-varying disturbances are generated from first-order Markov process $\dot{\tau}_{iw} = -\tau_{iw} + \lambda_i\omega_i$ [12], where $\tau_{iw} = [\tau_{iwu}, \tau_{iwv}, \tau_{iwr}]^T$, $\lambda_i = diag(\lambda_{1i}, \lambda_{2i}, \lambda_{3i})$ is a constant matrix, and ω_i is the Gaussian white noise. The parameters of sliding mode controllers are set as $c_{i1} = 1$, $k_i = 1$, $\eta_{i1} = 0.0000001$, $c_{i2} = 0.5$, and $\eta_{i2} = 0.000001$. The parameters of the FLS are set as $l = 1, \ldots, 5$, $[w_1, w_2, w_3, w_4, w_5]^T = [-1, -0.5, 0, 0.5, 1]^T$, $h_l = 0.5$, $\rho = 1, 2, 3$, $\gamma_{i1} = 1$, and $\gamma_{i2} = 1$. The lookahead distance is set as $\Delta_i = 3L$, where L is the length of ship. The reference surge velocity is set as $u_{id} = 5\text{m/s}$.

4.1. Three-Ship Cooperative Maritime Search Operation

In this section, the cooperative maritime search is conducted by three ships based on the presented improved RLOS guidance-based fuzzy sliding mode controller. The reference path for the cooperative maritime search is generated from the presented improved creeping line search method, which integrates the Bezier curve into the traditional creeping line search method to circumvent the transition points with corners and employs the cubic spline interpolation to produce a differentiable path. An improved RLOS guidance-based fuzzy sliding mode controller is used to control multiple ships to conduct the cooperative maritime search.

Sweep width is an important parameter in a maritime search operation. Thus, many experiments were conducted in different scenarios, and the table of sweep width was collected in [6]. In this section, consider a search scenario that the area is nearly 317 square kilometers, the length of ships to be searched is less than 5 m, and the visibility in current marine environment is 9 km. Then, the value of sweep width of the mentioned search scenario can be found in [6], and it is 2.6 km.

The cooperative maritime search is conducted by three ships, and the communication topology of ships is shown in Figure 5. The initial states of three ships are set as $[x_1(0), y_1(0), \psi_1(0), u_1(0), v_1(0), r_1(0)]^T = [0\text{ m}, 0\text{ m}, 0\text{ rad}, 0\text{ m/s}, 0\text{ m/s}, 0\text{ rad/s}]^T$, $[x_2(0), y_2(0), \psi_2(0), u_2(0), v_2(0), r_2(0)]^T = [0\text{ m}, 2600\text{ m}, 0\text{ rad}, 0\text{ m/s}, 0\text{ m/s}, 0\text{ rad/s}]^T$, $[x_3(0), y_3(0), \psi_3(0), u_3(0), v_3(0), r_3(0)]^T = [0\text{ m}, 5200\text{ m}, 0\text{ rad}, 0\text{ m/s}, 0\text{ m/s}, 0\text{ rad/s}]^T$.

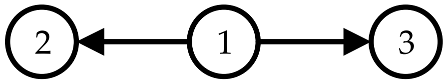

Figure 5. The communication topology of three ships.

Figures 6–9 give the simulations of the cooperative maritime search operation based on the presented improved creeping line search method under the mentioned search scenario. In Figure 6, the reference paths, which are denoted by purple line, brown line, and reddish-brown line, are generated by the presented improved creeping line search method by integrating the cubic spline interpolation into the Bezier curve. By this way, the transition points with corners in the traditional creeping line search method are circumvented, and the obtained reference paths are smooth and continuous. The yellow dotted line, orange dotted line, and olive-green dotted line are guidance paths, which are generated by improved RLOS guidance. Three ships are used to conduct the cooperative maritime search operation based on the presented improved RLOS guidance-based fuzzy sliding mode controller, and the green dotted line, red dotted line, and blue dotted line are the paths of three ships. The shapes of three ships, which are filled by green, red, and blue, are drawn in Figure 6 every 1000 s, and three ships can maintain the formation when they follow the straight part of the reference path and the curve part of the reference path. Figure 7 depicts the control inputs of three ships, which are generated by Equation (33) and Equation (41). There are some spikes in yaw moment, since the reference path is constituted by straight parts and curve parts, and ships need different heading angels to change their states when they travel from the straight part to the curve part, and vice versa. The values of control inputs of three ships are same since three ships have the same states, which satisfies that three ships can maintain their formation when they conduct the cooperative search. Considering unknown model dynamics and time-varying disturbances, the FLS with approximate ability is incorporated into the design of controllers, and the performance of fuzzy approximators is shown in Figures 8 and 9. The solid lines are approximated results of the FLS, and dotted lines are unknown model dynamic and time-varying disturbances. From Figures 8 and 9, it can be concluded that the FLS can approximate the unknown nonlinear function; although, the values of f_{ir} and f_{iu} are small and time-varying.

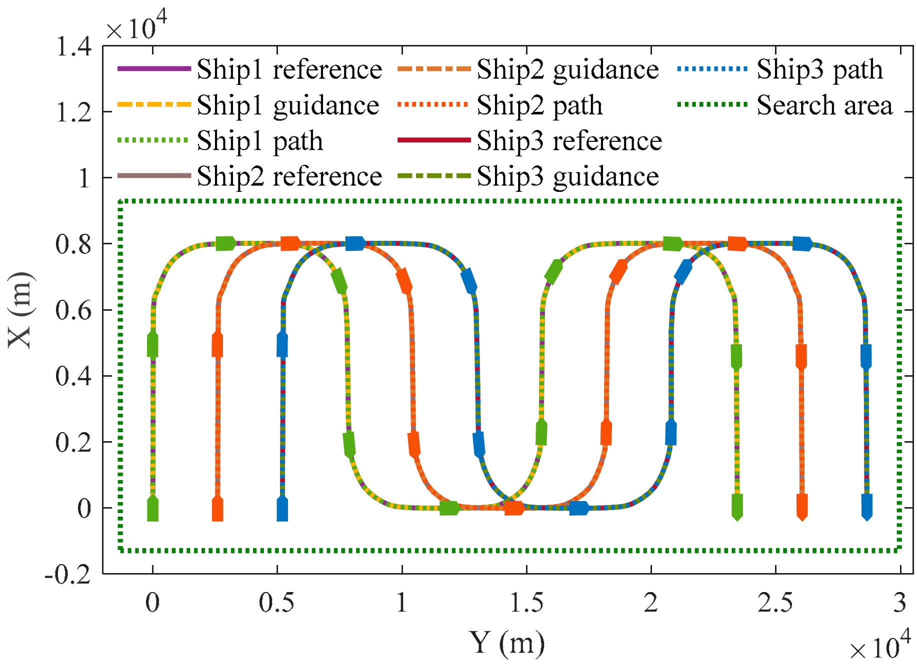

Figure 6. The performance of cooperative maritime search operation.

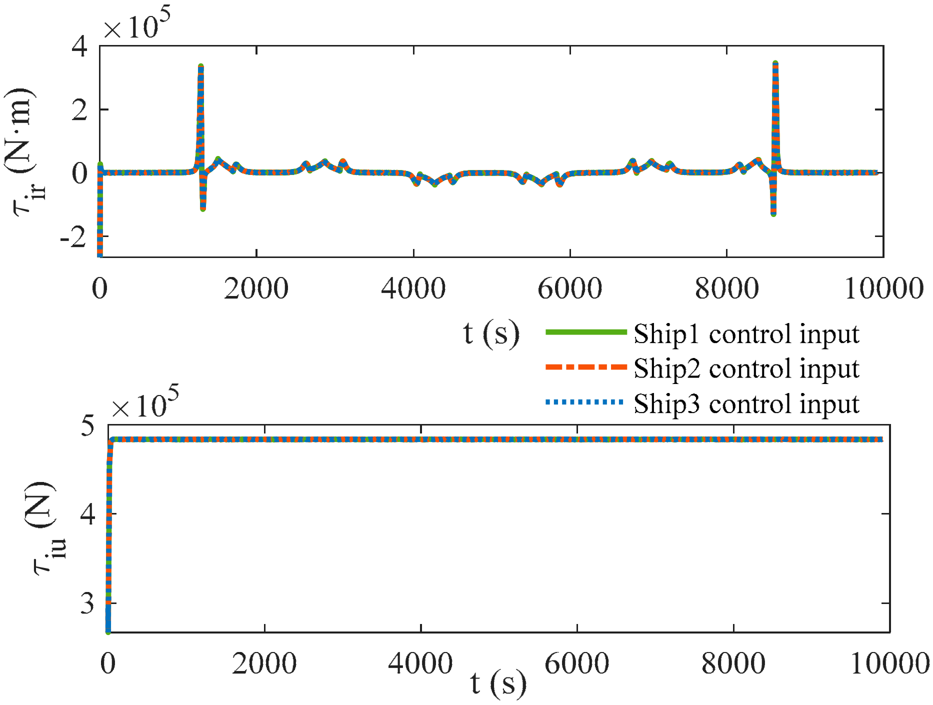

Figure 7. The control inputs of three ships.

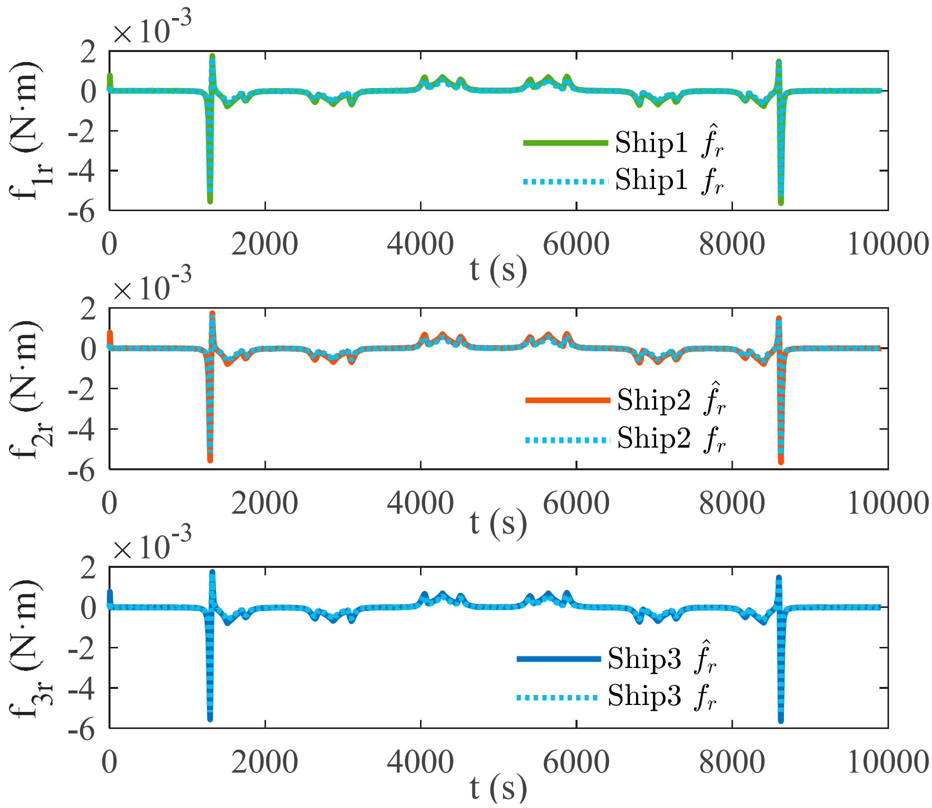

Figure 8. The approximated result of f_{ir}.

4.2. Comparative Studies between RLOS Guidance and Improved RLOS Guidance

In order to verify the effectiveness and advantages of the presented improved RLOS guidance, a comparative case between RLOS guidance and improved RLOS guidance was conducted. The straight-line path following of one underactuated ship was taken as an illustrated example. In practical applications, a kinematic discrepancy between the ship and its 3-DoF model usually exists, which is deserved to be noticed. RLOS guidance was presented to compensate this kinematic uncertainty based on the idea of sliding mode [18]; however, the existing chattering effect cannot be avoided. In order to improve the chattering effect, an improved RLOS guidance is presented for the first time based on the idea of robust adaptive control [22] in this paper.

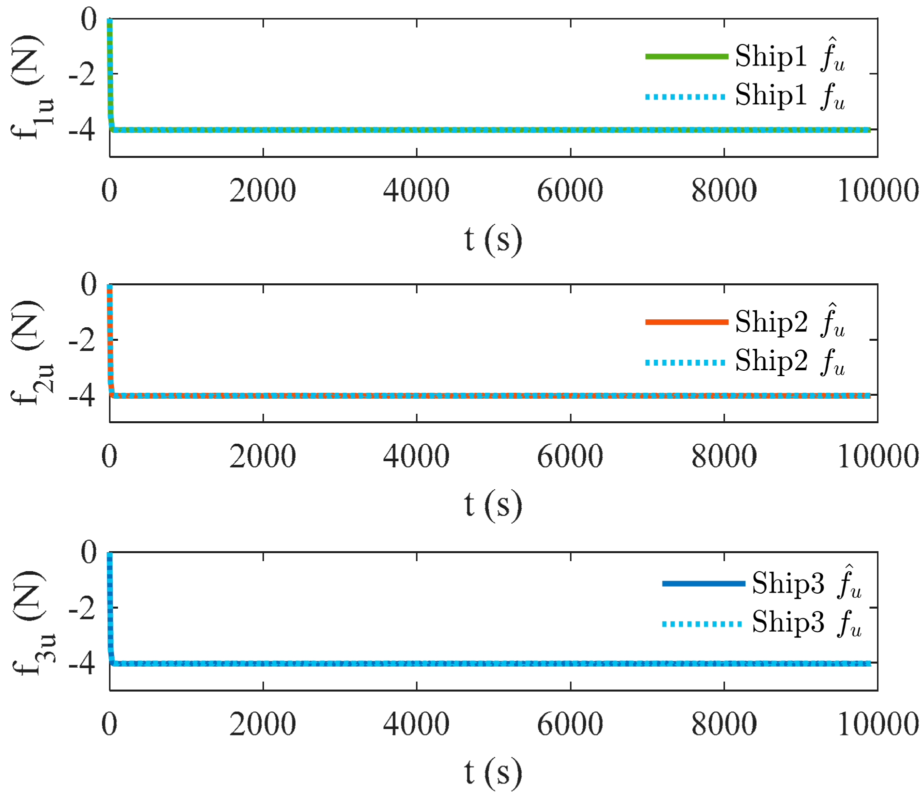

Figure 9. The approximated result of f_{iu}.

In order to verify the effectiveness of the presented improved RLOS guidance, a term $\xi(t) = 0.1 \sin t$ was added into the kinematic model, and the time-varying disturbances were ignored, i.e., $\tau_{iwu} = 0$, $\tau_{iwv} = 0$, and $\tau_{iwr} = 0$. The reference signal was given as

$$\begin{aligned} x_p(\zeta) &= x_0 + \zeta \cos \varpi \\ y_p(\zeta) &= y_0 + \zeta \sin \varpi \end{aligned} \tag{45}$$

where $x_0 = 0$, $y_0 = 1$, and $\varpi = \frac{\pi}{4}$. The initial states of the ship are set as $[x(0), y(0), \psi(0), u(0), v(0), r(0)]^T = [50\ \text{m}, 1\ \text{m}, 0\ \text{rad}, 0.1\ \text{m/s}, 0\ \text{m/s}, 0\ \text{rad/s}]^T$. The parameters of the RLOS guidance-based sliding mode controller and the improved RLOS guidance-based sliding mode controller are the same.

In Figure 10, the green line is the reference signal, which is generated by Equation (45). The yellow dotted line and the purple dotted line are guidance paths, which are generated by the RLOS guidance and the improved RLOS guidance. The orange dotted line and blue dotted line are ship paths based on the RLOS guidance-based sliding mode controller and improved RLOS guidance-based sliding mode controller. Figure 10 can show that the ship can follow the reference signal eventually. In Figure 11, the orange line is the control input of RLOS guidance-based sliding mode controller, and the blue dotted line is the control input of improved RLOS guidance-based sliding mode controller. In Figure 12, the along-track error x_e can converge to a small value because RLOS guidance and improved RLOS guidance can compensate the kinematic uncertainty between the ship and its 3-DoF model. Nevertheless, RLOS guidance compensates the kinematic uncertainty based on the idea of sliding mode [18], and the chattering effect cannot be avoided. Improved RLOS guidance is presented based on the idea of adaptive robust control; thus, the chattering effect is eased. It also shows that the along-track error x_e of the improve RLOS guidance is close to zero within 2 s, which is faster than the RLOS guidance.

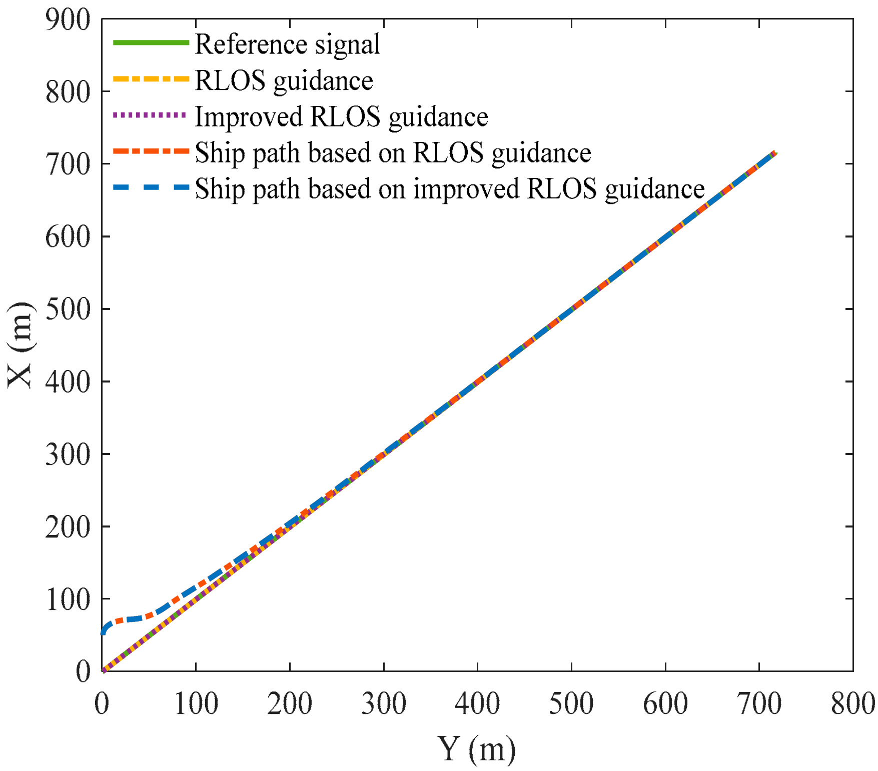

Figure 10. The straight-line path following.

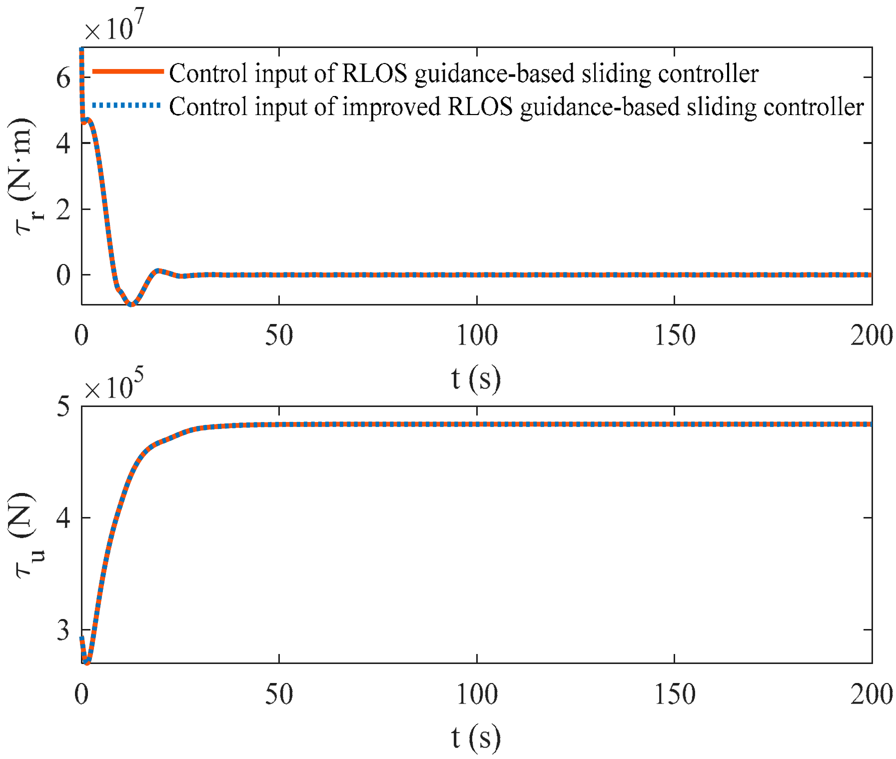

Figure 11. Control inputs of RLOS guidance-based sliding controller and improved RLOS guidance-based sliding controller.

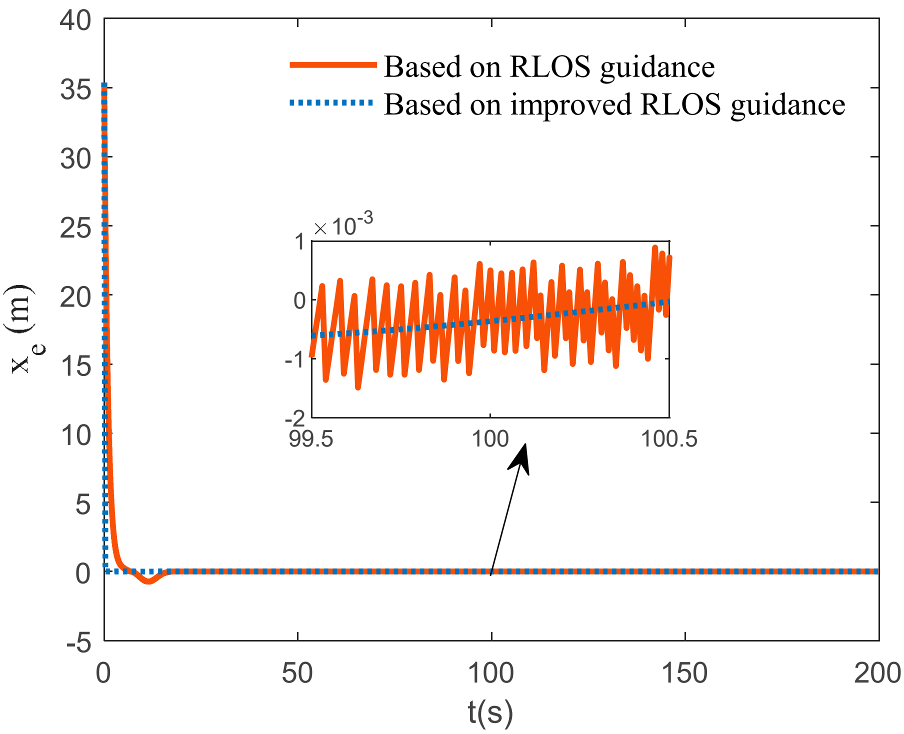

Figure 12. The comparison about x_e between RLOS guidance in [18] and improved RLOS guidance in this paper.

5. Conclusions

The improved RLOS guidance-based fuzzy sliding mode controller has been presented to control multiple underactuated ships to conduct the cooperative maritime search based on the presented improved creeping line search method in this paper. First, an improved creeping line search method is presented for the first time by integrating the Bezier curve into the traditional creeping line search method to circumvent the transition points with corners; then, the cubic spline interpolation is employed to connect these discrete points, which are generated by the Bezier curve. Compared with the traditional creeping line search method, the presented improved creeping line search method generates a smooth reference path. Second, an improved RLOS guidance is presented for the first time by exploring the idea of robust adaptive control, and the chattering effect of the RLOS guidance method is eased. Third, the fuzzy logic system is introduced to approximate the uncertain nonlinear model dynamics and time-varying disturbances. Finally, the improved RLOS guidance-based fuzzy sliding mode controller is presented. In the first simulation, three underactuated ships conduct the cooperative maritime search based on the presented improved creeping line search method under the improved RLOS guidance-based sliding mode controller, which can verify the effectiveness of the presented controller and the improved creeping lines search method. In the second comparative simulation between the presented improved RLOS guidance and RLOS guidance, the chattering effect of the RLOS guidance is eased by the presented improved RLOS guidance, and the advantages of the presented improved RLOS guidance method are shown. There is a central point in the communication topology, and the communication takes place before the cooperative maritime search operation. In future, the distributed maritime search will be researched, and ships will communicate with their neighbors instead of the central point in the process of the cooperative maritime search.

Author Contributions: Conceptualization, C.L.; Data curation, W.G.; Formal analysis, W.G. and C.L.; Funding acquisition, C.L.; Investigation, C.L.; Methodology, C.L.; Project administration, C.L.; Resources, C.L.; Software, W.G.; Supervision, C.L. and T.S.; Validation, W.G., C.L. and T.S.; Writing—original draft, W.G.; Writing—review and editing, C.L. and T.S. All authors have read and agreed to the published version of the manuscript.

Funding: This research was funded by the National Natural Science Foundation of China, grant number 52101397.

Institutional Review Board Statement: Not applicable.

Informed Consent Statement: Not applicable.

Data Availability Statement: The data that supports the funding of this study are available from the corresponding authors upon reasonable request.

Conflicts of Interest: The authors declare no conflicts of interest.

References

1. Walker, T.R.; Adebambo, O.; Feijoo, M.C.D.A.; Elhaimer, E.; Hossain, T.; Edwards, S.J.; Morrison, C.E.; Romo, J.; Sharma, N.; Taylor, S.; et al. Environmental effects of marine transportation. In *World Seas: An Environmental Evaluation*, 2nd ed.; Academic Press: London, UK, 2019.
2. Renga, A.; Graziano, M.D.; Moccia, A. Segmentation of marine SAR images by sublook analysis and application to sea traffic monitoring. *IEEE Trans. Geosci. Remote Sens.* **2019**, *57*, 1463–1477. [CrossRef]
3. Kang, C.M.; Yeh, L.C.; Jie, S.Y.R.; Pei, T.J.; Nugroho, H. Design of USV for search and rescue in shallow water. In Proceedings of the 13th International Conference on Intelligent Robotics and Applications, ELECTR Network, Kuala Lampur, Malaysia, 5–7 November 2020; pp. 351–363.
4. Kula, K.S. Automatic control of ship motion conducting search in open waters. *Pol. Marit. Res.* **2020**, *27*, 157–169. [CrossRef]
5. Mou, J.M.; Hu, T.; Chen, P.F.; Chen, L.Y. Cooperative MASS path planning for marine man overboard search. *Ocean Eng.* **2021**, *235*, 109376. [CrossRef]
6. International Maritime Organization and International Civil Aviation Organization (IMO/ICAO). *International Aeronautical and Maritime Search and Rescue Manual*; IMO/ICAO: London, UK, 1999.
7. Choi, J.W.; Curry, R.; Elkaim, G. Path planning based on Bezier curve for autonomous ground vehicles. In Proceedings of the Advances in Electrical and Electronics Engineering-IAENG Special Edition of the World Congress on Engineering and Computer Science 2008, San Francisco, CA, USA, 22–24 October 2008; pp. 158–166.
8. Miller, A.; Walczak, S. Maritime autonomous surface ship's path approximation using Bezier curves. *Symmetry* **2020**, *12*, 1704. [CrossRef]
9. McKinley, S.; Levine, M. Cubic spline interpolation. *Coll. Redw.* **1998**, *45*, 1049–1060.
10. Fossen, T.I. *Marine Control Systems—Guidance, Navigation, and Control of Ships, Rigs and Underwater Vehicles*; Marine Cybernetics: Trondheim, Norway, 2002.
11. Breivik, M.; Fossen, T.I. Principles of guidance-based path following in 2D and 3D. In Proceedings of the 44th IEEE Conference on Decision and Control, Seville, Spain, 12–15 December 2005; pp. 627–634.
12. Liu, L.; Wang, D.; Peng, Z.H. Path following of marine surface vehicles with dynamical uncertainty and time-varying ocean disturbances. *Neurocomputing* **2016**, *173*, 799–808. [CrossRef]
13. Liu, L.; Wang, D.; Peng, Z.H. ESO-based line-of-sight guidance law for path following of underactuated marine surface vehicles with exact sideslip compensation. *IEEE J. Ocean. Eng.* **2017**, *42*, 477–487. [CrossRef]
14. Zhang, G.Q.; Zhang, X.K.; Zheng, Y.F. Adaptive neural path-following control for underactuated ships in fields of marine practice. *Ocean Eng.* **2015**, *104*, 558–567. [CrossRef]
15. Shojaei, K. Neural adaptive robust control of underactuated marine surface vehicles with input saturation. *Appl. Ocean Res.* **2015**, *53*, 267–278. [CrossRef]
16. Yu, C.Y.; Liu, C.H.; Lian, L.; Xiang, X.B.; Zeng, Z. ELOS-based path following control for underactuated surface vehicles with actuator dynamics. *Ocean Eng.* **2019**, *187*, 106139. [CrossRef]
17. Liu, C.; Hu, Q.Z.; Sun, T. Distributed formation control of underactuated ships with connectivity preservation and collision avoidance. *Ocean Eng.* **2022**, *263*, 112350. [CrossRef]
18. Liu, C.; Guo, W.L.; Sun, T. RLOS-based path following with event-triggered roll motion control for underactuated ship using rudder. *Ocean Eng.* **2023**, *269*, 113592. [CrossRef]
19. Li, M.C.; Guo, C.; Yu, H.M.; Yuan, Y. Line-of-sight-based global finite-time stable path following control of unmanned surface vehicles with actuator saturation. *ISA Trans.* **2022**, *125*, 306–317. [CrossRef]
20. Do, K.D.; Jiang, Z.P.; Pan, J. Robust adaptive path following of underactuated ships. *Automatica* **2004**, *40*, 929–944. [CrossRef]
21. Su, Y.X.; Wan, L.L.; Zhang, D.H.; Huang, F.R. An improved adaptive integral line-of-sight guidance law for unmanned surface vehicles with uncertainties. *Appl. Ocean Res.* **2021**, *108*, 102488. [CrossRef]

22. Polycarpou, M.M.; Ioannou, P.A. A robust adaptive nonlinear control design. *Automatica* **1996**, *34*, 423–427. [CrossRef]
23. Utkin, V.; Guldner, J.; Shi, J. *Sliding Mode Control in Electro-Mechanical Systems*, 2nd ed.; CRC Press: Boca Raton, FL, USA, 2017.
24. Shtessel, Y.; Edwards, C.; Fridman, L.; Levant, A. *Sliding Mode Control and Observation*; Springer: New York, NY, USA, 2014.
25. Zhang, Y.; Liu, Y. Guidance-based path following of an underactuated ship based on Event-triggered sliding mode control. *J. Mar. Sci. Eng.* **2022**, *10*, 1780. [CrossRef]
26. Sun, T.; Liu, C.; Wang, X.G. Distributed anti-windup NN-sliding mode formation control of multi-ships with minimum cost. *ISA Trans.* **2023**, *138*, 49–62. [CrossRef]
27. Ren, Y.; Zhang, L.; Huang, W.; Chen, X. Neural Network-Based Adaptive Sigmoid Circular Path-Following Control for Underactuated Unmanned Surface Vessels under Ocean Disturbances. *J. Mar. Sci. Eng.* **2023**, *11*, 2160. [CrossRef]
28. Chen, X.; Liu, Z.; Zhang, J.Q.; Zhou, D.C.; Dong, J. Adaptive sliding-mode path following control system of the underactuated USV under the influence of ocean currents. *J. Syst. Eng. Electron.* **2018**, *29*, 1271–1283.
29. Tong, S.C.; Li, Q.G.; Chai, T.Y. Fuzzy adaptive control for a class of nonlinear systems. *Fuzzy Sets Syst.* **1999**, *101*, 31–39. [CrossRef]
30. Sui, S.; Chen, C.L.P.; Tong, S.C. Fuzzy adaptive finite-time control design for nontriangular stochastic nonlinear systems. *IEEE Trans. Fuzzy Syst.* **2019**, *27*, 172–184. [CrossRef]
31. Deng, Y.J.; Zhang, X.K.; Zhang, G.Q. Fuzzy logic based speed optimization and path following control for sail-assisted ships. *Ocean Eng.* **2019**, *171*, 300–310.
32. Zhang, G.Q.; Li, J.Q.; Liu, C.; Zhang, W.D. A robust fuzzy speed regulator for unmanned sailboat robot via the composite ILOS guidance. *Nonlinear Dyn.* **2022**, *110*, 2465–2480. [CrossRef]
33. Nei, J.; Lin, X.G. Improved adaptive integral line-of-sight guidance law and adaptive fuzzy path following control for underactuated MSV. *IAS Trans.* **2019**, *94*, 151–163.